

Time Resolved Photoluminescence of Si-doped High Al Mole Fraction AlGa_N Epilayers Grown by Plasma-Enhanced Molecular Beam Epitaxy

Madalina Furis, Alexander N. Cartwright, Jeonghyun Hwang¹ and William J. Schaff¹,
Department of Electrical Engineering, University at Buffalo,
Buffalo, NY, 14260, USA

¹ Department of Electrical Engineering, Cornell University,
Ithaca, NY, 14853 USA

ABSTRACT

We report on detailed temperature dependent, time-resolved photoluminescence (TRPL) studies of Si-doped AlGa_N epilayers. In these samples, the Al concentration varies from 25% to 66%. The samples were found to exhibit metallic-like temperature-independent conductivity. The deep level "yellow" emission, whose presence would indicate the existence of a large number of defects associated with growth, Si incorporation, and/or alloy formation, is absent. In addition to emission corresponding to the donor-bound exciton, the PL spectrum exhibits features associated with transitions involving localized carriers. This assignment of the emission mechanisms is based on the activation energies extracted from the temperature dependent photoluminescence (PL) quenching. Specifically, at room temperature the PL spectrum is dominated by transitions involving localized states. The localization energy varied from sample to sample and was observed to be between 115 meV to 200 meV. The PL intensity decay in the lower Al mole fraction epilayers exhibits a slow component associated with the presence of donor-bound excitons.

INTRODUCTION

Despite the significant progress made in the development of UV emitters, the fabrication of UV LEDs and laser diodes remains a challenging problem due, in part, to the difficulties encountered in the growth of high Al content AlGa_N. Ultimately, AlGa_N materials must be grown with reduced defect densities and high levels of both n- and p-type doping. Achieving very high electron concentration in high Al content AlGa_N is difficult due to formation of compensating deep acceptor states generated by the Ga or Al vacancies (V_{Ga}) [1,2] and oxygen DX centers [3]. As a result, AlGa_N doped with Si reaches a conductive state only for Si concentration exceeding 10^{18}cm^{-3} . [4]

A significant number of studies have been dedicated to increasing the n-type doping levels in AlGa_N[4-6] as well as studying the nature of the compensating acceptors[7,8], DX centers[1,3,9], and Si donors[6,7,10] in these alloys through transport and/or PL studies. Optical studies are especially important for highly doped AlGa_N epilayers that exhibit a metallic behavior even at room temperature[6,7], such as the ones studied by Hwang et al. [6] who reported temperature independent electron concentrations as high as $1.25 \times 10^{20}\text{cm}^{-3}$ in $\text{Al}_{0.5}\text{Ga}_{0.5}\text{N}$ and $8.5 \times 10^{19}\text{cm}^{-3}$ in $\text{Al}_{0.8}\text{Ga}_{0.2}\text{N}$ epilayers grown by rf plasma-enhanced molecular beam epitaxy.

The present work is an attempt to identify the origins of donor and acceptor states in samples studied by Hwang et al. through temperature dependent photoluminescence studies. A detailed fitting procedure allows the separation of the different components of the PL spectra and

the energies associated with the PL intensity quenching are identified with various donors and or acceptor binding energies. The donor bound exciton recombination is found to dominate the spectrum of the low Al mole fraction epilayers at low temperatures. The presence of a very shallow Si donor (binding energy equal to a few meV) is identified. Time-resolved photoluminescence measurements are used to estimate the carrier lifetime dependence on temperature in these epilayers.

EXPERIMENTAL DETAILS

The Si-doped AlGaIn epilayers were grown in a turbomolecular Varian Gen II MBE system which uses standard effusion cells for the group III elements. An EPI RF plasma source was used for the nitrogen source and 2 in. sapphire wafers with c-plane orientation were used as substrates. After loading into the growth chamber, each wafer was nitrided by nitrogen plasma at 200 °C for 30 min. and then heated at 830 °C for AlN nucleation layer growth. The Si-doped AlGaIn wafers with different Al mole fractions and Si fluxes were grown at 800 °C after the deposition of a 200 Å AlN buffer layer. The growth rate was almost the same for all wafers, 4000 Å/h. The Al mole fraction was subsequently determined by x-ray measurements. The thickness of all epilayers is 4000 Å and they are completely relaxed. A complete series of epilayers with Al mole fractions varying between $x = 0.25$ and $x = 1$ were grown through this method. Since the shortest excitation wavelength available for the studies presented here was 266 nm, our photoluminescence studies were limited to Al mole fractions smaller than 65%. All the samples, with the exception of the 52% Al mole fraction epilayer, exhibit metallic conductivity up to room temperature with measured Hall carrier concentrations in excess of 10^{18} cm^{-3} and as high as $1.25 \times 10^{20} \text{ cm}^{-3}$. More details about the growth process and transport measurements results can be found in reference [6]. Preliminary SIMS measurements show that, in addition to silicon, oxygen is present in the sample in concentrations as high as $3.4 \times 10^{19} \text{ cm}^{-3}$.

Time-resolved photoluminescence (TRPL) spectra were obtained using conventional time-correlated techniques. The 800 nm, 200 fs pulses from a Coherent 250 KHz repetition rate regenerative amplifier (REGA) were frequency tripled to provide a 250 fs, 266 nm pulsed excitation beam with an average power of 5 mW. The excitation beam was focused onto the sample to a diameter of approximately 60 μm . The luminescence signal was dispersed by a Chromex 250IS monochromator and detected by a Hamamatsu C4334 streak camera with a temporal jitter of 50 ps. The carrier lifetimes were estimated using an exponential fit to the observed decay data. For the temperature dependent photoluminescence studies, the samples were placed inside a closed cycle refrigerator. The temperature studies were carried out from 15 K to 300 K.

RESULTS AND DISCUSSION

A summary of the PL spectra from the samples under study is presented in Figure 1(a). The spectra taken at low temperatures (continuous lines) exhibit more than one feature at energies lower than the epilayer band gap (marked by arrows in the same figure). The red shift of the highest energy feature in the spectra with respect to the bandgap varies from approximately 30 meV in the low Al mole samples to hundreds of meV in the higher Al concentration epilayers. The spectrum of the 65% sample could not be recorded in its entirety since the highest excitation energy available for this experiment is lower than the nominal bandgap of $\text{Al}_{0.65}\text{Ga}_{0.35}\text{N}$. The

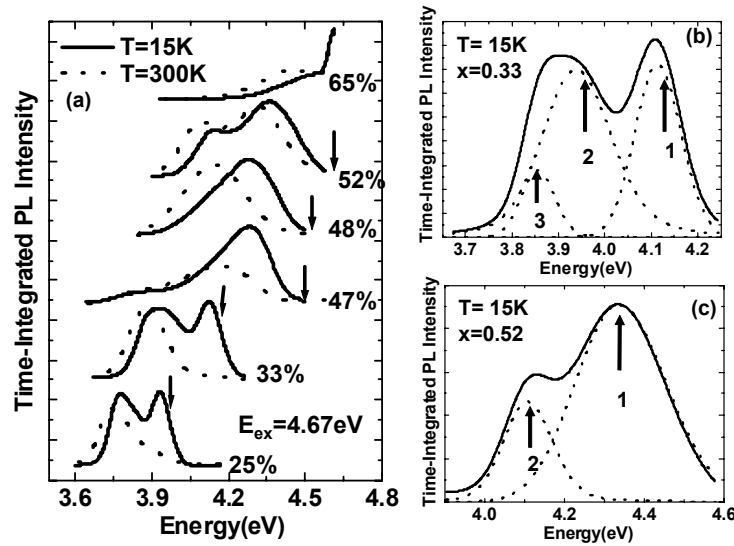


Figure 1 (a) PL spectra from the samples under study taken at 15K (solid lines) and room temperature (dashed lines), (b) Curve fitting of the 15K PL spectrum of sample AL33 using Voigt functions and (c) same fitting for sample AL52.

shape of the spectra changes significantly as the temperature increases such that, in some cases, the feature that dominated the spectrum at low temperature is absent at room temperature (dotted lines). None of the samples exhibit any deep level (yellow) luminescence.

The change in the relative intensity as a function of temperature between the various components in the PL spectra implies the features present in the spectra originate in different recombination mechanisms. This observation suggests a reliable interpretation of the PL spectra from the AlGaIn epilayers can be afforded only if each of the components is isolated through a fitting procedure and its temperature dependence is analyzed.

The results of a fitting carried out using Voigt functions for the PL spectra of samples containing 33% and 52% Al are plotted in Figure 1(b) and (c). The continuous lines represent the measured spectrum and the dotted curves are the components fitted to the spectrum. In some cases (for example the 33% or the 25% Al epilayers) a good fitting was obtained using three functions whereas in others (e.g. the 52% Al sample) two components were enough to obtain a good fit to the spectrum.

Next, the integrated intensity of each component was plotted as a function of inverse temperature in an Arrhenius plot and the activation energies associated with the quenching of each component were extracted from the plot, by fitting the intensity dependence on temperature with:

$$I(T) = \frac{I_0}{1 + \sum_i C_i \exp\left(-\frac{EA_i}{k_B T}\right)} \quad (1)$$

where I_0 represents the time-integrated intensity at low temperatures, and $i = 1, 2$ or 3 , depending on how many activation energies are associated with each component. The Arrhenius plots for the 25% sample are shown in Figure 2.

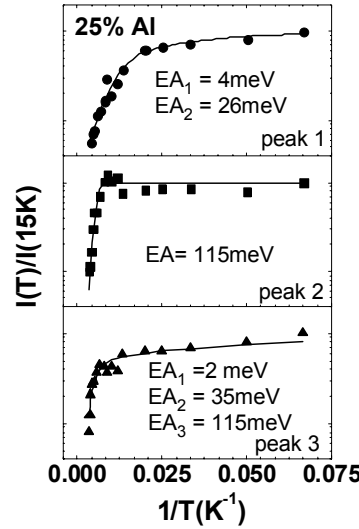


Figure 2 Photoluminescence intensity dependence on temperature for the three transitions identified in the PL spectrum of $\text{Al}_{0.25}\text{Ga}_{0.75}\text{N}$. The activation energies associated with peak 1 indicate this transition is associated with the radiative recombination of donor bound excitons. The presence of a very shallow donor is also identified.

For the highest energy peak (peak 1) the thermal quenching is characterized by two activation energies equal to 5 meV and 26 meV. These energies match the donor bound exciton and free exciton binding energies respectively, suggesting the highest energy feature in the spectrum corresponds to the radiative recombination of donor bound excitons at low temperatures and free excitons at higher temperatures. A similar behavior is encountered in the 33% Al sample where peak 1 is also characterized by a low activation energy, of the same order of the PL redshift with respect to the bandgap. In contrast, the second and third peak in the low Al mole fraction samples as well as the PL spectra in the high Al mole fraction samples are characterized by at least one activation energy larger than 100 meV. (around 115 meV for the 15% and 33% Al samples and 200 meV for the 47%, 48% and 52% Al samples).

The most straight forward approach is to identify the large activation energies with binding energies of shallow acceptors. Such acceptors have been observed in GaN[11], but their origins remain obscure. We cannot exclude the possibility that Si is substituting for N as well as Ga, thus acting like an acceptor or the formation of Si clusters with an acceptor character[12]. For the samples exhibiting metallic conductivity the presence of acceptors associated with the formation of $\text{V}_{\text{Ga}}\text{Si}_{\text{Ga}}$ complexes is also possible. [8]

In addition to donor bound excitons and conduction band to acceptor-related features, the photoluminescence spectra contain contributions from donor to acceptors transitions. (for example peak 3 in the 25% Al epilayer). The activation energies associated with the donor levels involved in these transitions range between 2 meV and 36 meV. Such low numbers indicate the possible formation of band-tail donor like states, almost resonant to the conduction band, and explains the metallic character observed in these samples.

Measurements of the PL intensity decay at different energies across the spectrum confirm the different nature of the recombination mechanisms. Since the epilayers are very thick and completely relaxed, only the recombination of carriers located at the AlN/AlGa_{0.75}N interface and possibly the surface recombination [13] are affected by the presence of spontaneous and piezoelectric polarization. Since the present experiment probes the recombination processes inside the epilayer, such effects can be neglected in the context of the present discussion. The

photoluminescence intensity decay as a function of time in the 25% Al sample is plotted in Figure 3 at three different temperatures and for two different energies. All curves can be fitted by a single exponential with the exception of the decay corresponding to the conduction band to acceptor transition (3.789 eV) decay at low temperatures, which is characterized by two distinct lifetimes. The most interesting aspect of the PL decay at this particular energy is, that the high injection lifetime (measured at early decay times to be 1.1 ns in this sample) is longer than the low injection (measured at longer decay times) lifetime and not vice versa, as expected. This behavior is encountered only for the donor to acceptor pair recombination in samples that also exhibit excitonic recombination. In contrast all, donor to acceptor transitions in the higher Al mole fraction samples are characterized by a single exponential decay.

A qualitative explanation for this behavior can be given if we consider that, in a very rough approximation, at low temperatures all non-radiative recombination channels are frozen and the donor-bound excitons recombine leaving the donor in its neutral state. In such a case, at early delay times, the loss of neutral donors through the donor to acceptor pair recombination is compensated by the generation of neutral donors resulting from the exciton recombination. This competition slows the donor-to-acceptor recombination process. Once most of the donor-bound excitons have recombined, the donor to acceptor pair recombination happens on a faster scale.

Temperature studies support this explanation. Figure 3(b) shows that at temperatures above 150 K, where most of the donor-bound excitons no longer exist, (their binding energy equals 5 meV) the slow component disappears as well. Moreover, this slow component has only been observed in the 25% and 33% epilayers, which are the only samples exhibiting a donor-bound exciton related feature in the PL spectrum at low temperatures.

CONCLUSIONS

Component-resolved TRPL studies of Si doped AlGaIn epilayers with different Al mole fractions have revealed the presence of a very shallow donor state (binding energy equal to only a few meV). The PL spectra contain several features associated with recombination of donor-bound exciton, conduction band to acceptor and donor-to-acceptor pair recombination. The origins of the acceptor states are still unclear. The slow photoluminescence intensity decay measured at

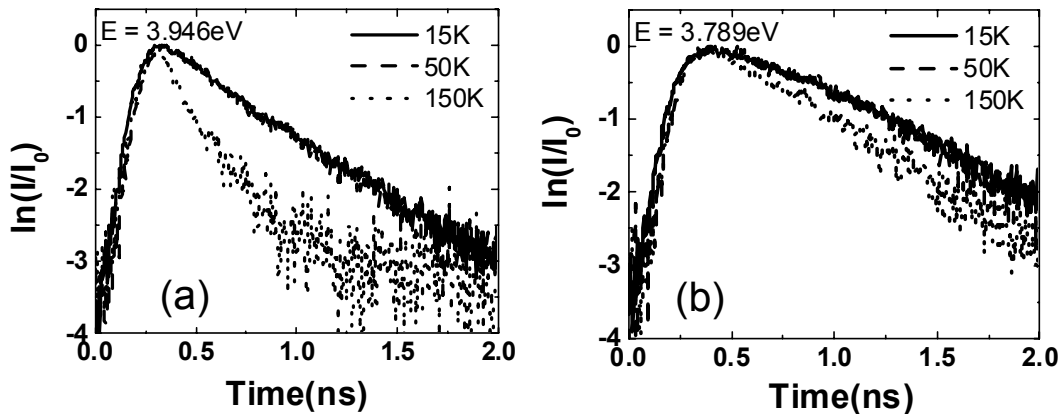


Figure 3 Photoluminescence intensity decay at 15K, 50K, and 150K for the 25%Al sample measured at energies corresponding to the excitonic transition (plot(a)) and donor to acceptor transition (plot(b)). The latter exhibits a slow decay component at low temperatures. The same decay becomes mono-exponential at 150K.

early decay times and energies corresponding to the donor –to-acceptor transition in the low Al mole fraction epilayers is associated with the existence of donor-bound excitons at low temperatures in these samples.

ACKNOWLEDGEMENTS

This work was supported in part by ANC's NSF CAREER Grant #9733720, ONR YIP Grant #N00014-00-1-0508, a Defense University Research Initiative on Nanotechnology Grant #F496200110358 through the Air Force Office of Scientific Research, and WJS's NSF Grant #ECS-0123453 and DARPA through Army Research Office Grant #DAAD19-02-0199.

REFERENCES

1. C. Stampfl and C. G. Van de Walle, *Applied Physics Letters* **72** (4), 459 (1998).
2. T. Mattila and R. M. Nieminen, *Physical Review B* **55** (15), 9571 (1997).
3. M. D. McCluskey, N. M. Johnson, C. G. Van de Walle, D. P. Bour, M. Kneissl, and W. Walukiewicz, *Physical Review Letters* **80** (18), 4008 (1998).
4. K. B. Nam, J. Li, M. L. Nakarmi, J. Y. Lin, and H. X. Jiang, *Applied Physics Letters* **81** (6), 1038 (2002).
5. H. Amano and I. Akasaki, *Optical Materials* **19** (1), 219 (2002); D. Korakakis, H. M. Ng, M. Misra, W. Grieshaber, and T. D. Moustakas, *Mrs Internet Journal of Nitride Semiconductor Research* **1** (1-46), art. no. (1996); M. Pophristic, S. P. Guo, and B. Peres, *Applied Physics Letters* **82** (24), 4289 (2003).
6. J. H. Hwang, W. J. Schaff, L. F. Eastman, S. T. Bradley, L. J. Brillson, D. C. Look, J. Wu, W. Walukiewicz, M. Furis, and A. N. Cartwright, *Applied Physics Letters* **81** (27), 5192 (2002).
7. A. Y. Polyakov, M. Shin, J. A. Freitas, M. Skowronski, D. W. Greve, and R. G. Wilson, *Journal of Applied Physics* **80** (11), 6349 (1996).
8. M. A. Reshchikov, H. Morkoc, S. S. Park, and K. Y. Lee, *Applied Physics Letters* **81** (26), 4970 (2002).
9. R. Zeisel, M. W. Bayerl, S. T. B. Goennenwein, R. Dimitrov, O. Ambacher, M. S. Brandt, and M. Stutzmann, *Physical Review B* **61** (24), R16283 (2000).
10. A. Y. Polyakov, N. B. Smirnov, A. V. Govorkov, M. G. Mil'vidskii, J. M. Redwing, M. Shin, M. Skowronski, D. W. Greve, and R. G. Wilson, *Solid-State Electronics* **42** (4), 627 (1998).
11. M. A. Reshchikov and R. Y. Korotkov, *Physical Review B* **64** (11), art. no. 115205 (2001); D. C. Reynolds, D. C. Look, B. Jogai, and R. J. Molnar, *Journal of Applied Physics* **89** (11), 6272 (2001); G. B. Ren, D. J. Dewsnip, D. E. Lacklison, J. W. Orton, T. S. Cheng, and C. T. Foxon, *Materials Science and Engineering B-Solid State Materials for Advanced Technology* **43** (1-3), 242 (1997).
12. T. Sato and T. Ishiwatari, *Journal of Applied Physics* **91** (8), 5158 (2002).
13. O. Ambacher, J. Majewski, C. Miskys, A. Link, M. Hermann, M. Eickhoff, M. Stutzmann, F. Bernardini, V. Fiorentini, V. Tilak, B. Schaff, and L. F. Eastman, *Journal of Physics-Condensed Matter* **14** (13), 3399 (2002).